

<sup>1</sup> Institut Pluridisciplinaire Hubert Curien, UMR 7178, CNRS-IN2P3 and Université de Strasbourg, B.P. 28, F-67037 Strasbourg Cedex 2, France

<sup>2</sup> China Institute of Atomic Energy (CIAE), 102413 Beijing, China

# Multi-neutron transfer coupling in sub-barrier $^{32}\text{S} + ^{90,96}\text{Zr}$ fusion reactions

A. RICHARD<sup>1</sup>, C. BECK<sup>1</sup>, H.Q. ZHANG<sup>2</sup>, C.J. LIN<sup>2</sup>, F. YANG<sup>2</sup>, H.M. JIA<sup>2</sup>, X.X. XU<sup>2</sup>, Z.D. WU<sup>2</sup>, F. JIA<sup>2</sup>, S.T. ZHANG<sup>2</sup>, Z.H. LIU<sup>2</sup>

The role of neutron transfers is investigated in the fusion process below the Coulomb barrier by analyzing  $^{32}\text{S}+^{90}\text{Zr}$  and  $^{32}\text{S}+^{96}\text{Zr}$  as benchmark reactions. A full coupled-channel calculation of the fusion excitation functions has been performed for both systems by using multi-neutron transfer coupling for the more neutron-rich reaction. The enhancement of fusion cross sections for  $^{32}\text{S}+^{96}\text{Zr}$  is well reproduced at sub-barrier energies by NTFus code calculations including the coupling of the neutron-transfer channels following the Zagrebaev semiclassical model. We found similar effects for  $^{40}\text{Ca}+^{90}\text{Zr}$  and  $^{40}\text{Ca}+^{96}\text{Zr}$  fusion excitation functions.

## 1. Introduction

Heavy-ion fusion reactions with colliding neutron-rich nuclei at bombarding energies at the vicinity and below the Coulomb barrier have been widely studied [1, 2, 3, 4, 5, 6, 7, 8, 9, 10]. The specific role of multi-step neutron-transfers in sub-barrier fusion enhancement still needs to be investigated in detail both experimentally [2, 5, 9] and theoretically [4, 6]. In a complete description of the fusion dynamics the transfer channels in standard coupled-channel (CC) calculations [1, 4, 6, 10, 11] have to be taken into account accurately. It is known that neutron transfers may induce a neck region of nuclear matter in-between the interacting nuclei favoring the fusion process to occur.

In low-energy fusion reactions, the very simple one-dimensional barrier-penetration model (1D-BPM) is based upon a real potential barrier resulting from the attractive nuclear and repulsive Coulomb interactions. For light- and medium-mass nuclei, one only assumes that the di-nuclear system fuses as soon as it has reached the region inside the barrier i.e. within the potential pocket. If the system can evolve with a bombarding energy high enough to pass through the barrier and to reach this pocket with a reasonable amount of energy, the fusion process will occur after a complete amalgamation of the colliding nuclei forming the compound nucleus. On the other hand, for

sub-barrier energies the di-nuclear system has not enough energy to pass through the barrier. In this case, neutron pick-up processes can occur when the nuclei are close enough to interact each other significantly [3, 4], if the Q-values of neutron transfers are positive.

It was shown that sequential neutron transfers can lead to the broad distributions characteristic of many experimental fusion cross sections. Finite Q-value effects can lead to neutron flow and a build up of a neck between the target and projectile [4]. The situation of this neck formation of neutron matter between the two colliding nuclei could be considered as a “doorway state” to fusion. In a basic view, this intermediate state induced a barrier lowering. As a consequence, it will favor the fusion process at sub-barrier energies and enhance significantly the fusion cross sections. Experimental results have already shown such enhancement of the sub-barrier fusion cross sections due to the neutron-transfer channels with positive Q-values [2, 5].

## 2. Experimental results

In order to investigate the role of neutron transfers we further study  $^{32}\text{S} + ^{90}\text{Zr}$  and  $^{32}\text{S} + ^{96}\text{Zr}$  as benchmark reactions. Fig. 1 displays the measured fusion cross sections for  $^{32}\text{S} + ^{90}\text{Zr}$  (open circles) and  $^{32}\text{S} + ^{96}\text{Zr}$  (points). We present the analysis of excitation functions of evaporation residues (ER) cross sections recently measured with high precision (i.e. with small energy steps and good statistical accuracy for these reactions [12]).

The differential cross sections of quasi-elastic scattering (QEL) at backward angles were previously measured by the CIAE group [9]. The analysis of the corresponding BD-QEL barrier distributions (see solid points in Fig. 2) already indicated the significant role played by neutron transfers in the fusion processes.

In Fig. 2 we introduce the experimental fusion-barrier (BD-Fusion) distributions (see open points) obtained for the two reactions by using the three-point difference method of Ref. [4] as applied to the data points of Ref. [12] plotted in Fig. 1. It is interesting to note that in both cases the BD-Fusion and BD-QEL barrier distributions are almost identical up to  $E_{c.m.} \approx 85$  MeV.

## 3. Coupled channel analysis

We have developed a new CC computer code named NTFus [13] by taking the neutron transfer channels into account in the framework of the semiclassical model of Zagrebaev [6]. We will show that the effect of the neutron transfer channels yields a fairly good agreement with the present data of sub-barrier fusion cross sections measured for  $^{32}\text{S} + ^{96}\text{Zr}$ , the more

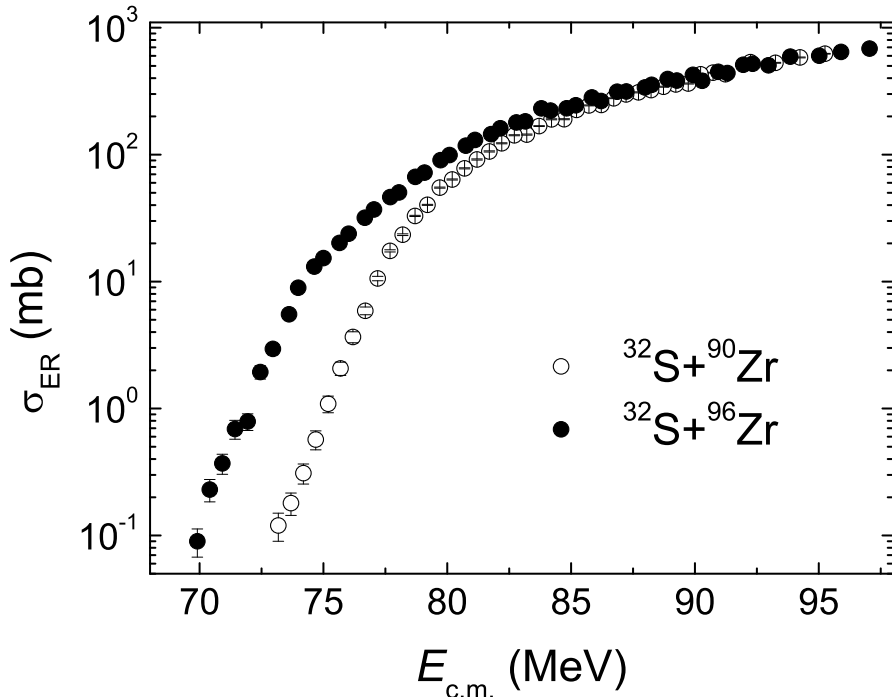


Fig. 1. Comparison between the fusion-evaporation (ER) excitation functions of  $^{32}\text{S} + ^{90}\text{Zr}$  (open circles) and  $^{32}\text{S} + ^{96}\text{Zr}$  (points) as a function of the center-of-mass energy. The error bars of the experimental data taken from Ref. [12] represent purely statistics uncertainties.

neutron-rich reaction [12]. This was initially expected from the positive  $Q$ -values of the neutron transfers as well as from the failure of standard CC calculation of quasi-elastic barrier distributions without neutron-transfers coupling [9] as shown by the solid line in Fig. 2(b).

By fitting the present experimental fusion excitation function given in Fig. 1 with NTFus CC calculation [13], we will be able to conclude that the effect of the neutron transfer channels produces the rather significant enhancement of the sub-barrier fusion cross sections of  $^{32}\text{S} + ^{96}\text{Zr}$  as compared to  $^{32}\text{S} + ^{90}\text{Zr}$ .

A detailed inspection of the  $^{32}\text{S} + ^{90}\text{Zr}$  fusion data presented in Fig. 1 along with the negative  $Q$ -values of their corresponding neutron transfer channels lead us to speculate with the absence of a neutron transfer effect on the sub-barrier fusion for this reaction. We proceed step by step by performing calculations for this reaction with the NTFus code [13] (see Fig. 3).

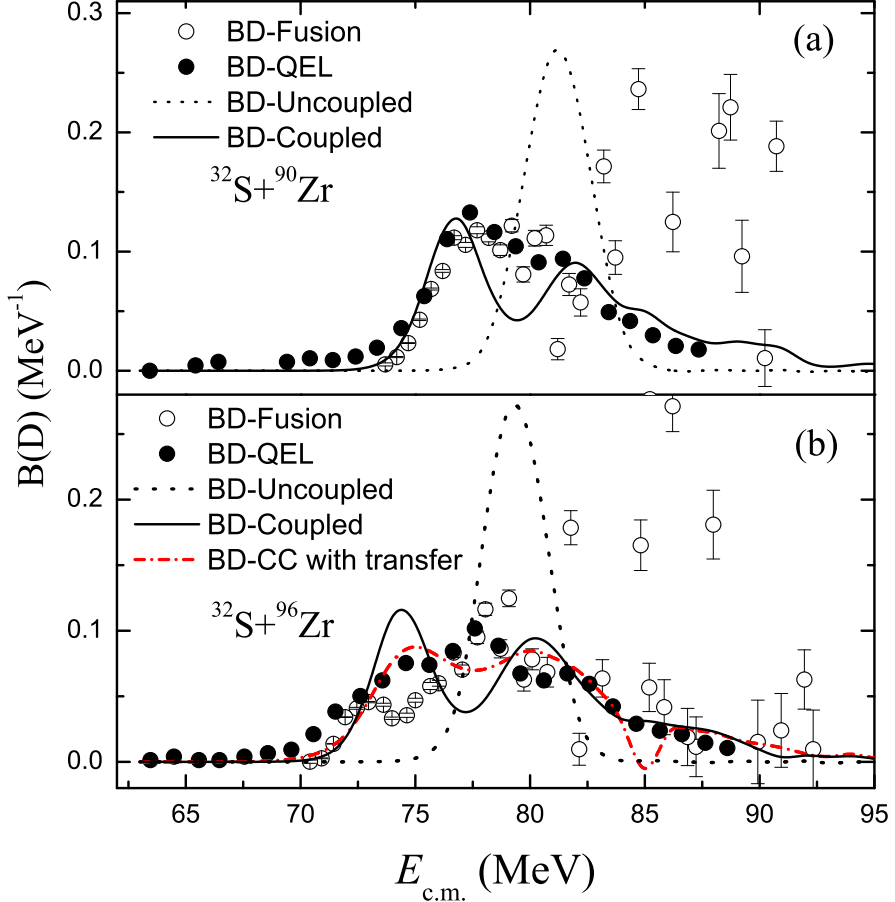


Fig. 2. Barrier distributions (BD) from the fusion ER (open circles) cross sections [12], plotted in Fig.1, and quasielastic scattering (solid circles) cross sections [9] for  $^{32}\text{S} + ^{90}\text{Zr}$  (a) and  $^{32}\text{S} + ^{96}\text{Zr}$  (b). The dashed and solid black lines represent uncoupled calculations (1D-BPM) and the CC calculations without neutron transfer coupling. The red dash-dotted line represents the CC calculations with neutron transfer coupling for the  $^{32}\text{S} + ^{96}\text{Zr}$  reaction.

#### 4. NTFus CC calculations for $^{32}\text{S} + ^{90,96}\text{Zr}$

With the semiclassical model developed by Zagrebaev [6] we propose in the following discussion to definitively demonstrate the significant role of neutron transfers for the  $^{32}\text{S} + ^{96}\text{Zr}$  fusion reaction by fitting its experimental excitation function with NTFUS code [13] calculations, as shown in Fig. 4. The main characteristics of the code are briefly described thereafter.

The new oriented object NTFus code [13], using the Zagrebaev model [6] was implemented (at the CIAE) in C++, using the compiler of ROOT [14], following the basic equations of Ref. [15].

Let us first remind the values chosen for the deformation parameters and the excitation energies that are given in Table 1 [1, 16, 17]. The quadrupole vibrations of both the  $^{90}\text{Zr}$  and  $^{96}\text{Zr}$  are weak in energy; they lie at comparable energies.

Table 1. Excitation energies  $E_x$ , spins and parities  $\lambda^\pi$  and deformation parameters  $\beta_\lambda$  from [1, 16, 17].

Nucleus	$E_x$ (MeV)	$\lambda^\pi$	$\beta_\lambda$
$^{32}\text{S}$	2.230	$2^+$	0.32
	5.006	$3^-$	0.40
$^{90}\text{Zr}$	2.186	$2^+$	0.09
	2.748	$3^-$	0.22
$^{96}\text{Zr}$	1.751	$2^+$	0.08
	1.897	$3^-$	0.27

The  $^{96}\text{Zr}$  nucleus presents a complicated situation [18]: its low-energy spectrum is dominated by a  $2^+$  state at 1.748 MeV and by a very collective  $[B(E3;3^- \rightarrow 0^+) = 51 \text{ W.u.}]$   $3^-$  state at 1.897 MeV. CC calculations explained the larger sub-barrier enhancement as due mainly to the strong octupole vibration of the  $3^-$  state in  $^{36}\text{S} + ^{96}\text{Zr}$  [19]. However, the agreement is not so satisfactory below the barrier for  $^{32}\text{S} + ^{96}\text{Zr}$  (see solid line of Fig. 4), as well as for  $^{40}\text{Ca} + ^{96}\text{Zr}$  [5] and, therefore, there is the need to take neutron transfers into account.

The main functions of the code NTFus are designed to calculate the fusion excitation functions with normalized barrier distribution (based on experimental data) given by CCFULL [11], we take the dynamical deformations into account.

To take into account the neutron transfers, the NTFus code [13] applies the Zagrebaev model [6] to calculate the fusion cross sections  $\sigma_{fus}(E)$  as a function of center-of-mass energy  $E$ . Then the fusion excitation function can be derived using the following formula [6]:

$$T_l(E) =$$

$$\int f(B) \frac{1}{N_{tr}} \sum_k \int_{-E}^{Q_0(k)} \alpha_k(E, l, Q) \times P_{HW}(B, E + Q, l) dQ dB. \quad (1)$$

and

$$\sigma_{fus}(E) = \frac{\pi\hbar^2}{2\mu E} \sum_{l=0}^{l_{cr}} (2l+1) T_l(E). \quad (2)$$

where  $T_l(E)$  are the transmission coefficients,  $E$  is the energy given in the center-of-mass system,  $B$  and  $f(B)$  are the barrier height and the normalized barrier distribution function,  $P_{HW}$  is the usual Hill-Wheeler formula.  $l$  is the angular momentum whereas  $l_{cr}$  is the critical angular momentum as calculated by assuming no coupling (well above the barrier).  $\alpha_k(E, l, Q)$  and  $Q_0(k)$  are, respectively, the probabilities and the Q-values for the transfers of  $k$  neutrons. And  $1/N_{tr}$  is the normalization of the total probability taking into account the neutron transfers.

The NTFUS code [13] uses the ion-ion potential between two deformed nuclei as developed by Zagrebaev and Samarin in Ref. [15]. Either the standard Woods-Saxon form of the nuclear potential or a proximity potential [20] can be chosen. The code is also able to predict fusion cross sections for reactions induced by halo projectiles; for instance  ${}^6\text{He} + {}^{64}\text{Zn}$  [21]. In the following, only comparisons for  ${}^{32}\text{S} + {}^{90}\text{Zr}$  and  ${}^{32}\text{S} + {}^{96}\text{Zr}$  are discussed.

For the high-energy part of the  ${}^{32}\text{S} + {}^{90}\text{Zr}$  excitation function, one can notice a small over-estimation of the fusion cross sections at energies above the barrier up to the point used to calculate the critical angular momentum. This behavior can be observed at rather high incident energies - i.e. between about 82 MeV and 90 MeV (shown in Fig. 3 for  ${}^{32}\text{S} + {}^{90}\text{Zr}$  reaction). We want to stress that the corrections do not affect our conclusions that the transfer channels have a predominant role below the barrier for  ${}^{32}\text{S} + {}^{96}\text{Zr}$  reaction, as shown in Fig. 4.

As expected, we obtain a good agreement with calculations not taking any neutron transfer coupling into account for  ${}^{32}\text{S} + {}^{90}\text{Zr}$  as shown by the solid line of Fig. 3 (the dashed line are the results of calculations performed without any coupling). On the other hand, there is no significant over-estimation at sub-barrier energies. As a consequence, it is possible to observe the strong effect of neutron transfers on the fusion for the  ${}^{32}\text{S} + {}^{96}\text{Zr}$  reaction at sub-barrier energies. Moreover, the barrier distribution function  $f(B)$  extracted from the data contains the information of the neutron transfers. These information are also contained in the transmission coefficients, which are the most important parameters for the fusion cross sections to be calculated accurately. The  $f(B)$  function as calculated with the three-point formula [4] will mimic the differences induced by the neutron transfer taking place in sub-barrier energies where the cross section variations are very small (only visible if a logarithm scale is employed for the fusion excitation function). It is interesting to note that the Zagrebaev model [6] implies a modification of the Hill-Wheeler probability and does not concern the bar-

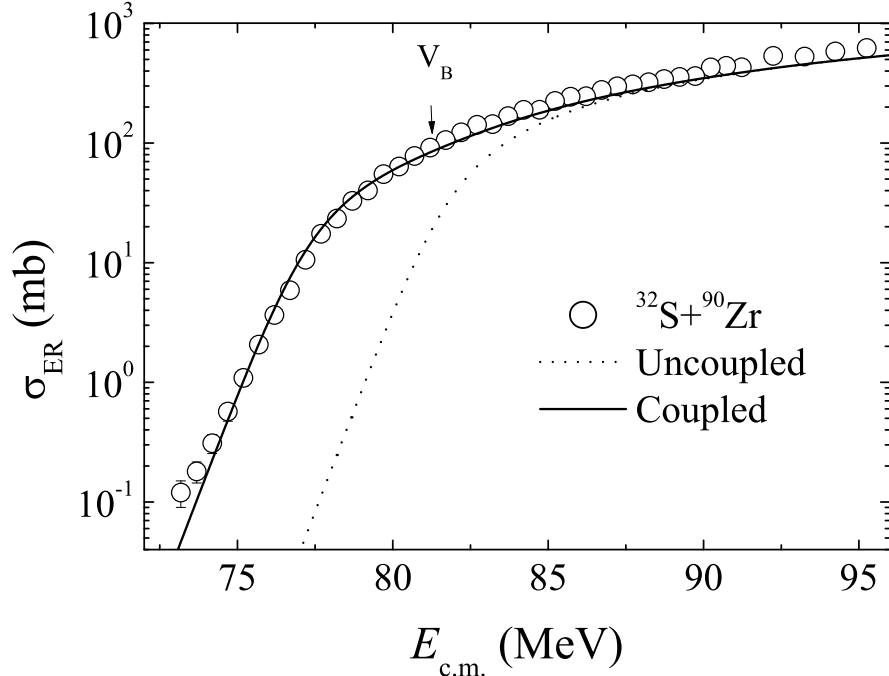


Fig. 3. Fusion-evaporation (ER) excitation function for  $^{32}\text{S}+^{90}\text{Zr}$ . The solid points are the experimental data [12] (see Fig.1). The dashed and solid lines are the uncoupled calculations, and CC calculations without neutron transfers, respectively. The arrow indicates the position of the Coulomb barrier for  $^{32}\text{S}+^{90}\text{Zr}$  as given by the 1D-BPM model (see Fig. 2).

rier distribution function  $f(B)$ . Finally, the code allows us to perform each calculation by taking the neutron transfers into account or not.

Table 2. Q-values in MeV for neutron pickup transfer channels from ground state to ground state for  $^{32}\text{S}+^{90}\text{Zr}$  and  $^{32}\text{S}+^{96}\text{Zr}$ , respectively.

System	+1n	+2n	+3n	+4n
$^{32}\text{S}+^{90}\text{Zr}$	-3.33	-1.229	-6.59	-6.319
$^{32}\text{S}+^{96}\text{Zr}$	0.788	5.737	4.508	7.655

The calculation with the neutron transfer effect is performed here up to the channel +4n ( $k=4$ ), but we have seen that we obtain the same overall agreement with data up to channels +5n and +6n. The Q-values and the separation energies for the  $^{96}\text{Zr}$  nucleus used for this calculation (solid line in Fig. 4) are displayed in the Tables 2 and 3, respectively.

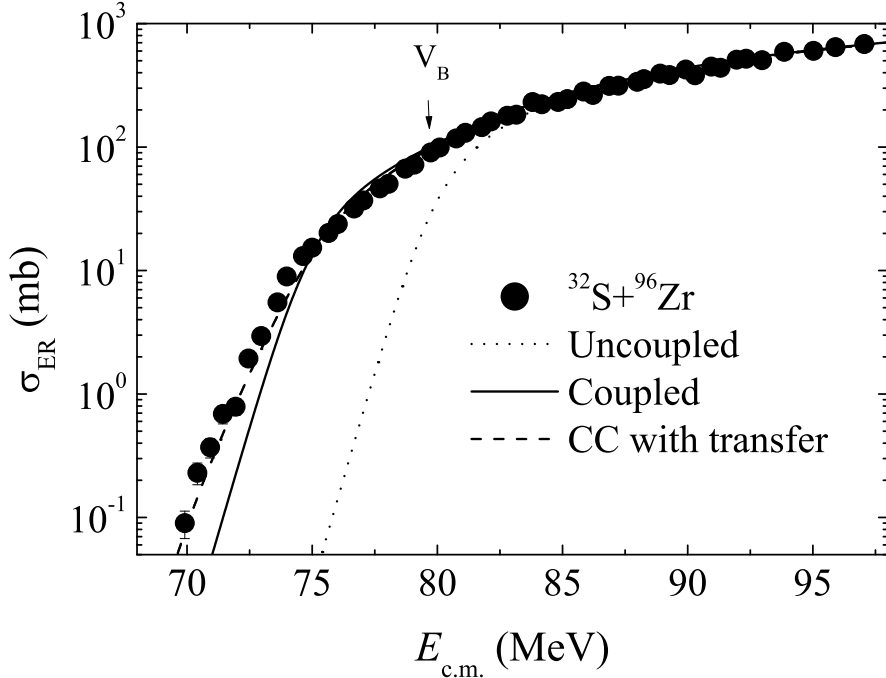


Fig. 4. Fusion-evaporation (ER) excitation function for  $^{32}\text{S} + ^{96}\text{Zr}$ . The solid points are the experimental data [12] (see Fig.1). The dashed, solid, and dotted lines are the uncoupled calculations, and CC calculations without and with neutron transfers, respectively. The arrow indicates the position of the Coulomb barrier for  $^{32}\text{S} + ^{96}\text{Zr}$  as given by the 1D-BPM model (see Fig. 2).

Table 3. Separation energies in MeV of each neutron for  $^{96}\text{Zr}$ .  
 $1^{\text{st}}$  neutron     $2^{\text{nd}}$  neutron     $3^{\text{rd}}$  neutron     $4^{\text{th}}$  neutron

7.854	6.463	8.230	6.733
-------	-------	-------	-------

As we can see on Fig. 4, the solid line representing standard CC calculations without the neutron transfer coupling (the dotted line is given for uncoupled calculations) does not fit the experimental data well at sub-barrier energies. On the other hand, the dotted line displaying NTFus calculations taking the neutron transfer coupling into account agrees perfectly well with the data. As expected, the Zagrebaev semiclassical model's correction applied at sub-barrier energies enhances the calculated cross sections. Moreover, it allows to fit the data reasonably well and therefore illustrates the strong effect of neutron transfers for the fusion of  $^{32}\text{S} + ^{96}\text{Zr}$ .

at subbarrier energies.

The present full CC analysis of  $^{32}\text{S} + ^{96}\text{Zr}$  fusion data [12] using NTFus [13] confirms perfectly well first previous CC calculations [6] describing well the earlier  $^{40}\text{Ca} + ^{90,96}\text{Zr}$  fusion data [5] and, secondly, very recent fragment- $\gamma$  coincidences measured for  $^{40}\text{Ca} + ^{96}\text{Zr}$  multi-neutron transfer channels [18].

### 5. Summary and conclusions

We have investigated the fusion process (excitation functions and extracted barrier distributions [12]) at near- and sub-barrier energies for the two neighbouring reactions  $^{32}\text{S} + ^{90}\text{Zr}$  and  $^{32}\text{S} + ^{96}\text{Zr}$ . For this purpose a new computer code named NTFus [13] has been developed by taking the coupling of the multi-neutron transfer channels into account by using the semiclassical model of Zagrebaev [6].

The effect of neutron couplings provides a fair agreement with the present data of sub-barrier fusion for  $^{32}\text{S} + ^{96}\text{Zr}$ . This was initially expected from the positive Q-values of the neutron transfers as well as from the failure of previous CC calculation of quasi-elastic barrier distributions without coupling of the neutron transfers [9]. With the agreement obtained by fitting the present experimental fusion excitation function and the CC calculation at sub-barrier energies, we conclude that the effect of the neutron transfers produces a rather significant enhancement of the sub-barrier fusion cross sections of  $^{32}\text{S} + ^{96}\text{Zr}$  as compared to  $^{32}\text{S} + ^{90}\text{Zr}$ . At this point we did not try to reproduce the details of the fine structures observed in the fusion barrier distributions. We believe that to achieve this final goal it will first be necessary to measure the neutron transfer cross sections to provide more information on the coupling strength of neutron transfer because its connection with fusion is not yet fully understood [18].

### 6. Acknowledgments

This work was supported by the National Natural Science Foundation of China under Grants No. 10575134, No. 10675169, and No. 10735100, and the Major State Basic Research Developing Program under a 2007 Grant No. CB815003. One of us (A.R.) thanks Region Alsace of France for the Boussole Grant 2009 No. 080105519 that was proposed to him during his six-month stay in 2009 at the CIAE, in Beijing, China.

### REFERENCES

- [1] M. Dasgupta, D.J. Hinde, N. Rowley, and A.M. Stefanini, Annu. Rev. Nucl. Part. Sci. **48**, 401 (1998).
- [2] R. Pengo *et al.*, Nucl. Phys. A **411**, 256 (1983),
- [3] P.H. Stelson, Phys. Lett. B **205**, 190 (1988).
- [4] N. Rowley *et al.*, Phys. Lett. B **282**, 276 (1992).
- [5] H. Timmers *et al.*, Nucl. Phys. **A633**, 421 (1998).
- [6] V.I. Zagrebaev, Phys. Rev. C **67**, 061601 (2003).
- [7] A.M. Stefanini *et al.*, Phys. Rev. C **73**, 034606 (2006).
- [8] A.M. Stefanini *et al.*, Phys. Rev. C **76**, 014610 (2007).
- [9] F. Yang, C.J. Lin, X.K. Wu, H.Q. Zhang, C.L. Zhang, P. Zhou, and Z.H. Liu, Phys. Rev. C **77**, 014601 (2008).
- [10] Sunil Kalkal *et al.*, Phys. Rev. C **81**, 044610 (2010).
- [11] K. Hagino, N. Rowley, and A.T. Kruppa, Comput. Phys. Commun. **123**, 143 (1999).
- [12] H.Q. Zhang *et al.*, Phys. Rev. C **82**, 054609 (2010).
- [13] H.Q. Zhang *et al.*, AIP Conf. Proc. **1235**, 50 (2010); A. Richard, C. Beck, H.Q. Zhang (in preparation).
- [14] <http://root.cern.ch>, website of ROOT.
- [15] V.I. Zagrebaev and V.V. Samarin, Physics of Atomic Nuclei **67** No.8, 1462 (2004).
- [16] S. Raman, C.W. Nestor, and P. Tikkainen, At. Data Nucl. Data Tables **78**, 1 (2001).
- [17] T. Kebedi and R.H. Spear, At. Data Nucl. Data Tables **89**, 77 (2005).
- [18] S. Szilner *et al.*, J. Phys.: Conf. Ser. **282**, 012021 (2011).
- [19] A.M. Stefanini *et al.*, Phys. Rev. C **62**, 014601 (2000).
- [20] J. Blocki, J. Randrup, W.J. Swiatecki, and C. F. Tsang, Annals of Physics **105**, 427 (1977).
- [21] M. Fisichella *et al.*, J. Phys.: Conf. Ser. **282**, 012014 (2011).